

Planar-surface charge densities and energies beyond the local-density approximation

Z. Y. Zhang* and David C. Langreth

Department of Physics and Astronomy, Rutgers University, Piscataway, New Jersey 08855-0849

John P. Perdew

Department of Physics and Quantum Theory Group, Tulane University, New Orleans, Louisiana 70118

(Received 7 October 1988)

We present a self-consistent calculation of the ground-state properties of simple metallic planar surfaces using density-functional theory with nonlocal exchange-correlation effects included. Our calculational scheme closely follows the classic work of Lang and Kohn for the jellium model, except that the exchange-correlation energy and potential within the local-density approximation (LDA) are replaced by the corresponding nonlocal functionals of Langreth and Mehl (LM). We also include the discrete-lattice effects, following the variational scheme of Perdew and Monnier. The physical properties considered include the one-electron effective potential, charge-density profile, surface energy, and work function. For each of the most densely packed surfaces of seven simple metals with fcc or bcc structure, we find that, when compared with results in the LDA, the Friedel oscillation in the electron density near the surface is systematically depressed as a result of positive LM contributions to the effective potential at places where the LDA density oscillation is peaked. We find a systematic increase in surface energies, with bigger increases for higher-density metals. Increases are also found in the work functions. Our results and those from other density-functional calculations are compared with results from variational treatments of the ground-state wave function, and with experiment. We also comment upon the Fermi hypernetted-chain jellium surface energies and work functions.

I. INTRODUCTION

Density-functional theory (DFT), following the pioneering work of Hohenberg, Kohn, and Sham,^{1,2} has proven to be very powerful for calculations of ground-state electronic properties of atoms, molecules, solids, and solid surfaces. Along the path of applying DFT with greater accuracy to a wide range of systems, various improvements to this theory have been developed. One such improvement is the nonlocal correction to the local-density approximation (LDA) for the exchange-correlation energy and potential developed by Langreth and Mehl^{3,4} using the wave-vector method of Langreth and Perdew.⁵ This correction, summarized by the Langreth-Mehl (LM) functional, has been tested on the ground-state properties of atoms,⁴ molecules,⁶⁻⁸ bulk materials,⁹⁻¹¹ and the linear potential model of a metal surface.^{4,12,13} Recently, its spin-dependent version¹⁴ has also been tested on several systems. Significant improvements over LDA have been found in most cases.

In this work, we present the first self-consistent Langreth-Mehl calculations for metal surfaces. We address not only the jellium model but also the simple real metals, to which we apply the variational treatment of discrete-lattice potentials developed by Perdew and Monnier.^{15,16}

Kohn-Sham density-functional theory was first applied to surfaces by Lang and Kohn (LK).¹⁷ In that classic work, self-consistent potentials and charge-density profiles at the surface were obtained for nine simple metals within the jellium model and the local-density approx-

imation. Also calculated were the surface energies, work functions,¹⁸ and image-plane positions,¹⁹ with the discrete-lattice potentials treated perturbatively. Later, Monnier and Perdew¹⁶ (MP) generalized the work of Lang and Kohn by treating the lattice potential in a variational self-consistent way. They found that, when compared with LK results, the charge-density oscillations at a given surface can be either enhanced or depressed, depending upon the sign of their single face-dependent variational parameter. They also found improved surface energies, which resulted mainly from the variational treatment of the lattice potential and partly from the inclusion of nonlocal contributions obtained in an early implementation of wave-vector analysis.²⁰⁻²²

Quite recently, as an alternative to the local-density approximation, a variational method with a trial ground-state wave function was applied to metal surfaces by two different groups²³⁻²⁵ using different calculational schemes. This approach is appealing because it does not assume for its *a priori* validity a slow spatial variation of the electronic density (unlike most density-functional approximations). One of the most distinctive results of the Fermi hypernetted-chain (FHNC) calculation²⁵ is the increase over LDA in the surface energy, with a larger increase for the higher-density metals. In the following, we show that a (somewhat smaller) increase in surface energy over LDA is also obtained if the LM nonlocal functionals are introduced into the density-functional treatment. Indications of such increases originating from nonlocal effects have been found earlier.²² A "back-of-the-envelope" estimate of the surface correlation energy is

deferred to Appendix A; this estimate gives values close to those obtained by the FHNC method. Appendix A also presents an improved estimate of the FHNC work function, and further comments on the surface energy.

After the LM nonlocality and the ionic potential¹⁶ are taken into account self-consistently, we find surface energies and work functions in reasonable agreement with experiment for most of the metals which we consider.

Another feature of the LM correction is its influence on electron density distributions at surfaces. When compared with LDA, the LM functional systematically depresses the density oscillation as judged by the height of the first Friedel peak just inside the jellium edge. This depression in electron density oscillation can be qualitatively understood from the fact that the LM correction in the exchange-correlation potential is always positive at the position of the peak. Such a positive correction pushes electrons away from the peak, suppressing the peak height.

II. METHOD

Since our calculations follow the scheme developed by Perdew and Monnier,^{15,16} which in turn was built upon the work of Lang and Kohn,^{17,18} we outline only those parts which are indispensable for the present discussion, and refer to the earlier work by these authors for a detailed description.

The total ground-state energy E of a system of electrons interacting with static ions can be written as a functional^{1,2} of the electron number density $n(\mathbf{r})$, one part of which is the exchange-correlation energy E_{xc} . To construct the electron density $n(\mathbf{r})$, one needs the one-electron wave functions ψ_i , which satisfy the self-consistent Schrödinger equation

$$\left[-\frac{\hbar^2}{2m}\nabla^2 + v_{\text{eff}}[n(\mathbf{r})] \right] \psi_i = \epsilon_i \psi_i, \quad (2.1)$$

$$n(\mathbf{r}) = \sum_i |\psi_i(\mathbf{r})|^2, \quad (2.2)$$

where the effective one-particle potential $v_{\text{eff}}[n(\mathbf{r})]$ is the sum of the ionic potential, the Coulomb potential from the other electrons, and the exchange-correlation potential given by $v_{xc}[n(\mathbf{r})] = \delta E_{xc}[n(\mathbf{r})] / \delta n(\mathbf{r})$, respectively:

$$v_{\text{eff}}[n(\mathbf{r})] = v(\mathbf{r}) + \int d\mathbf{r}' \frac{n(\mathbf{r}')}{|\mathbf{r} - \mathbf{r}'|} + v_{xc}[n(\mathbf{r})]. \quad (2.3)$$

When applied to a semi-infinite metal filling the half space $x < 0$, the first two terms on the right-hand side of (2.3) can be rewritten as $\phi[n(\mathbf{r})] + \delta v(\mathbf{r})$, where¹⁶

$$\phi[n(\mathbf{r})] = \int d\mathbf{r}' \frac{n(\mathbf{r}') - n_+(\mathbf{r}')}{|\mathbf{r} - \mathbf{r}'|}, \quad (2.4)$$

and $\delta v(\mathbf{r})$ is a perturbation arising from the effect of the discrete lattice. In (2.4), $n_+(\mathbf{r})$ is the density of the neutralizing positive background, which for the jellium model is defined as $n_+(\mathbf{r}) = \bar{n}\Theta(-x)$, where \bar{n} is the bulk average of $n(\mathbf{r})$. The unit step function $\Theta(-x)$ is 1 for $x < 0$, and 0 for $x > 0$.

One crucial difference between the work by Lang and

Kohn and that by Monnier and Perdew lies in their different ways of treating $\delta v(\mathbf{r})$. In the former work, $\delta v(\mathbf{r})$ was treated by first-order perturbation theory, while in the latter it was incorporated variationally in the self-consistent scheme for calculating the density and surface energy of the system. Monnier and Perdew¹⁶ tried two forms for doing the variation; for simplicity and consistency we will adopt only one, as both produced very similar results. In Ref. 16, a variational parameter C was introduced so that $C\Theta(-x)$ replaces $\delta v(\mathbf{r})$ in (2.1). Physically, positive C pushes electrons out into the vacuum region, while negative C has the opposite effect; $C=0$ reproduces the jellium-model result. The best value of C , denoted by C_m , is determined by minimizing the surface energy.

Our present calculation differs further from that of Monnier and Perdew (MP) in the approximation employed for exchange and correlation. MP used the Wigner interpolation formula²⁶ within the local-density approximation (LDA). They simply added to the LDA surface energy the nonlocal correction obtained from earlier work on wave-vector analysis,²⁰⁻²² which preceded the development of the LM functional. Here we include the local and the nonlocal contributions of the exchange-correlation potential *both* self-consistently, and examine the corresponding change in *each* of the physical quantities concerned, including the effective potential, the electron density profile, the surface energy, and so forth. We also reoptimize the parameter C .

We use the Langreth-Mehl (LM) functional^{3,4} to account for the nonlocal effects. We approximate E_{xc} by the sum of local and nonlocal contributions as

$$E_{xc}[n] = E_{xc}^{\text{local,RPA}}[n] + \int d\mathbf{r} n(\mathbf{r}) \epsilon_{xc}^{\text{nl,LM}}[n(\mathbf{r})], \quad (2.5)$$

where $\epsilon_{xc}^{\text{nl,LM}}[n(\mathbf{r})]$ is the LM nonlocal exchange-correlation energy density per particle:

$$\epsilon_{xc}^{\text{nl,LM}}[n(\mathbf{r})] = a \frac{[\nabla n(\mathbf{r})]^2}{[n(\mathbf{r})]^{7/3}} (2e^{-F - \frac{7}{9}}), \quad (2.6)$$

where

$$F = b \frac{|\nabla n(\mathbf{r})|}{[n(\mathbf{r})]^{7/6}}, \quad (2.7)$$

and in Rydberg atomic units (rydbergs and bohrs) the constants a and b are given by

$$a = \pi / [8(3\pi^2)^{4/3}] = 4.287 \times 10^{-3}, \quad (2.8)$$

$$b = (9\pi)^{1/6} f = 1.745 f, \quad (2.9)$$

with $f = 0.17$. We found that the sensitivity of the self-consistent results to f was about the same as that found by LM for the linear potential model,⁴ with smaller f 's still giving higher surface energies (see Appendix B). For the sake of consistency,^{4,14} a random-phase-approximation (RPA) expression must be used for the local contribution in (2.5), and in the present calculation we use the von Barth-Hedin (vBH) parametrization.²⁷

The corresponding LM exchange-correlation potential is

$$v_{xc}^{nl,LM}[n(\mathbf{r})] = 2an^{-1/3} \left\{ \frac{7}{9} \left[\frac{\nabla \cdot \mathbf{K}}{n} - \frac{2K^2}{3n^2} \right] - 2e^{-F} \left[\frac{(1-F/2)\nabla \cdot \mathbf{K}}{n} - \left(\frac{2}{3} - \frac{11F}{6} + \frac{7F^2}{12} \right) \frac{K^2}{n^2} + \frac{F(F-3)\mathbf{K} \cdot \nabla |\mathbf{K}|}{2n|\mathbf{K}|} \right] \right\}, \quad (2.10)$$

where $\mathbf{K} = \nabla n(\mathbf{r})$. The approximation for the potential given in (2.10) breaks down outside the charge distribution, where v_{xc} slowly becomes larger and eventually approaches infinity. This divergence has very little effect on the numbers obtained for the energy and density (except in the extreme tail), but presents numerical problems. We follow the procedure of cutting off this divergence at a value of x so large that the difference between a finite and infinite potential no longer has a noticeable effect. We implement this cutoff in the same way as in previous work,^{4,28} by multiplying (2.10) by a suppression factor $\exp(-h|\nabla n|^2 n^{-8/3})$. The calculations shown used $h = 10^{-4}$. We similarly suppress (2.6); the result is a slight increase (<1%) in the total surface energy (column 8, Table III). If a stronger suppression factor with $h = 2^{2/3} \times 10^{-3}$ were used for both (2.6) and (2.10), the total surface energies would increase further by amounts <2%.

III. RESULTS

A. Effective potential

For simplicity, we have considered only the most densely packed surfaces of the seven simple metals Al, Pb, Li, Na, K, Pb, and Cs. We show in Figs. 1–4 the corresponding change in the one-electron effective potential v_{eff} caused by LM nonlocality for the jellium surfaces of Al and K, and the real surfaces of Na(110) and Cs(110), respectively. Also shown are two of the contributing components: the electrostatic and the exchange-correlation potentials.

Figures 1 and 2, and the corresponding density distributions given later in Figs. 5 and 6, are chosen to make comparison with previous jellium-model calculations. From Figs. 1 and 2, we observe that in the surface region, the nonlocal LM contribution to v_{eff} gives mainly positive corrections inside the jellium edge, and negative corrections outside. These corrections are smaller in magnitude for higher-density metals, and are barely noticeable in Fig. 1 for Al. In particular, the LM corrections are always positive at places where the LDA density oscillation is peaked. The opposite was found by Ossicini *et al.*²⁹ using the Gunnarsson-Jones (GJ) nonlocal functional.³⁰

For real-metal surfaces where the variational parameter C is equal to C_m , the LM correction to v_{eff} is similar to that for jellium surfaces, as shown in Figs. 3 and 4. In particular, depression in Friedel oscillation due to LM persists as one passes from jellium to the real surface case.

At large distances outside the surface, the LDA and LM potentials do not behave correctly; there the image potential $-1/[4(x-x_0)]$ should be found, where x_0 is the position of the image plane. But the effect of this er-

ror on any of the physical quantities considered here is very small, since the image-potential behavior occurs at distances where the electron density is nearly zero. In Figs. 1–4, we use solid vertical lines to indicate the image-plane positions obtained from a formula fitted to LDA results for the centroid of excess charge [Eq. (8) of Ref. 31]. This formula is accurate enough to serve our present purpose, as any nonlocal effect is believed to be small.^{32–34} Clearly, the unphysically high values in both the exchange-correlation and the effective potentials, which arise from the breakdown of the LM, begin to develop well outside the image plane. For each of Figs. 1–4, we have stopped plotting both the nonlocal exchange-correlation and the total effective potentials at some distance away from the jellium edge; beyond this distance, the two potentials begin to be affected by the suppression factor introduced (see Sec. II) to simplify the numerics, and hence are not features of the LM method *per se*. We might mention that even with a much stronger suppression factor like $h = 2^{2/3} \times 10^{-3}$, which totally suppresses the unphysical increases in the potentials,

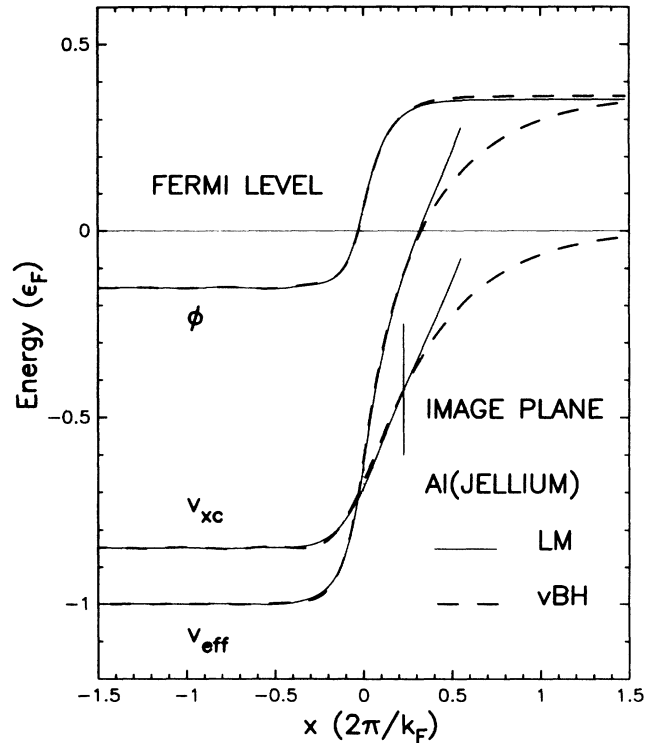


FIG. 1. The effective one-electron potential (v_{eff}) for a jellium surface with $r_s = 2.07$. Also shown are the classical electrostatic (ϕ) and exchange-correlation (v_{xc}) contributions. The dashed curves are calculated within the LDA (vBH); the solid curves contain the LM corrections. All energies are given in units of the Fermi energy, and plotted relative to the Fermi level. For details, see the text.

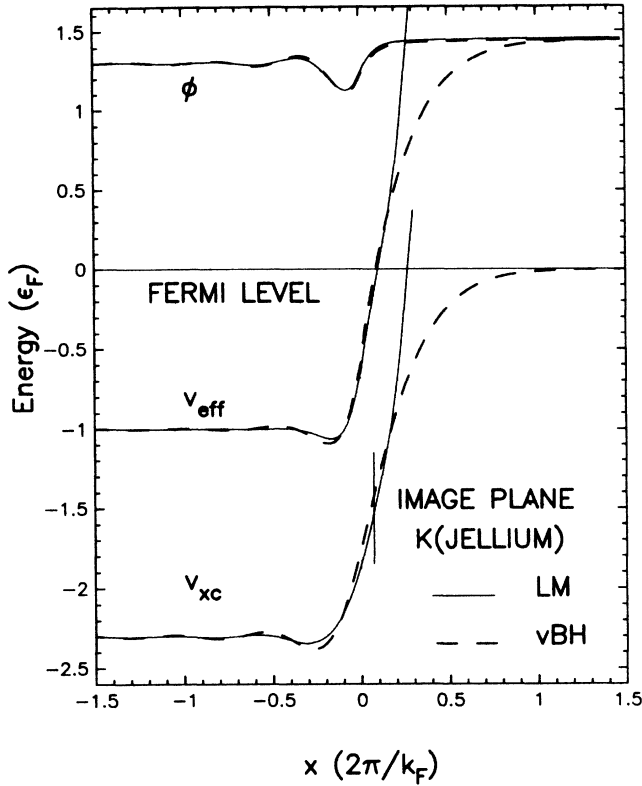


FIG. 2. Same as in Fig. 1, but for a jellium surface with $r_s = 4.96$.

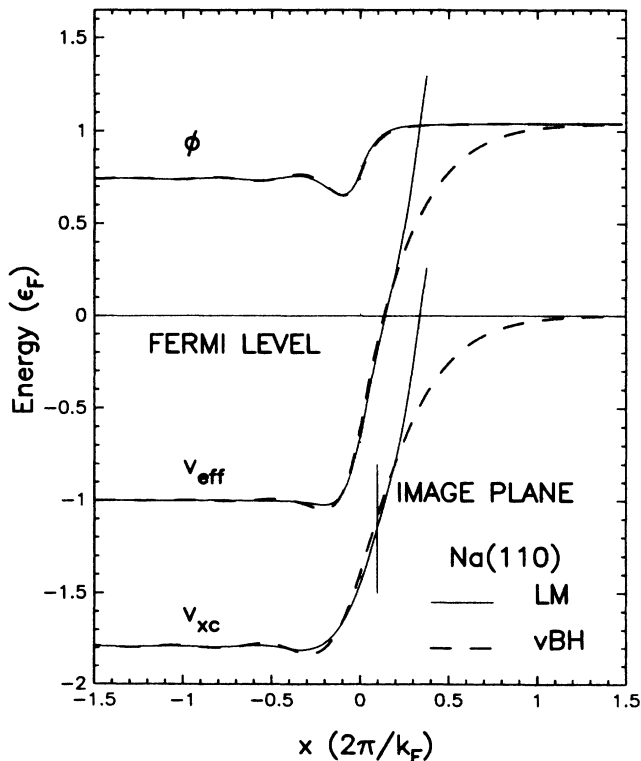


FIG. 3. Same as in Fig. 1, but for the real surface of Na [bcc (110) face, $C=0.15$ eV]. Here the step function $C_m \Theta(-x)$ in $v_{\text{eff}}(x)$ is present, but not clearly visible, because in this case C_m is a small fraction of ϵ_F . Cf. Fig. 4.

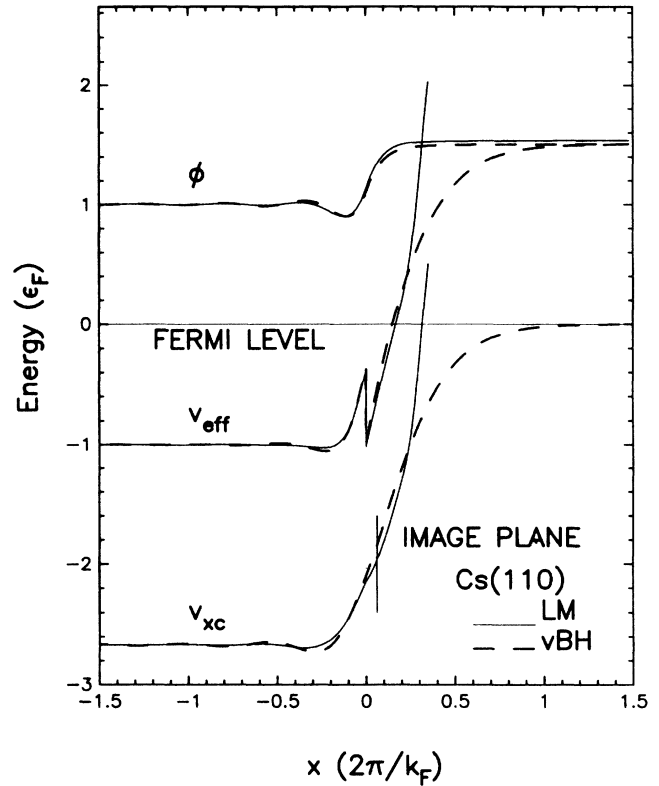


FIG. 4. Same as in Fig. 1, but for the real surface of Cs [bcc (110) face, $C=1.05$ eV].

the physical quantities of interest, including the charge-density distribution, the total surface energy, and the work function, would remain essentially unchanged. In their original work, Lang and Kohn¹⁷ checked the effect of combining the LDA up to the classical turning point with the correct asymptotic image potential, and found a very small correction to the LDA electron density. A similar small correction to our LM results is to be expected.

B. Electron density profile

In Figs. 5–8, we show the electron density profiles corresponding to the effective potentials shown in Figs. 1–4. For the two jellium surfaces of Al and K, we also show the difference between the nonlocal and local distributions. For either a jellium surface or a real surface, the depression in the Friedel oscillations in the surface region is apparent, and the physical reason for the depression can be qualitatively understood from the behavior of the potential, as explained in Sec. I. In fact, our density profile for $r_s = 4.96$ is very similar to that obtained by Krotscheck, Kohn, and Qian²⁵ (KKQ). For $r_s = 2.07$ the comparison is less clear, because KKQ reference their nonlocal-density calculation with the LDA at $r_s = 2.00$. At these densities we found that this r_s difference makes as large an effect on the density as the nonlocal correction. The reduction in Friedel oscillation strength which we find was also found by Sun *et al.*^{23,24} In contrast, in the calculation of Ossicini *et al.*,²⁹ an increase in density oscillation was found for every surface considered.

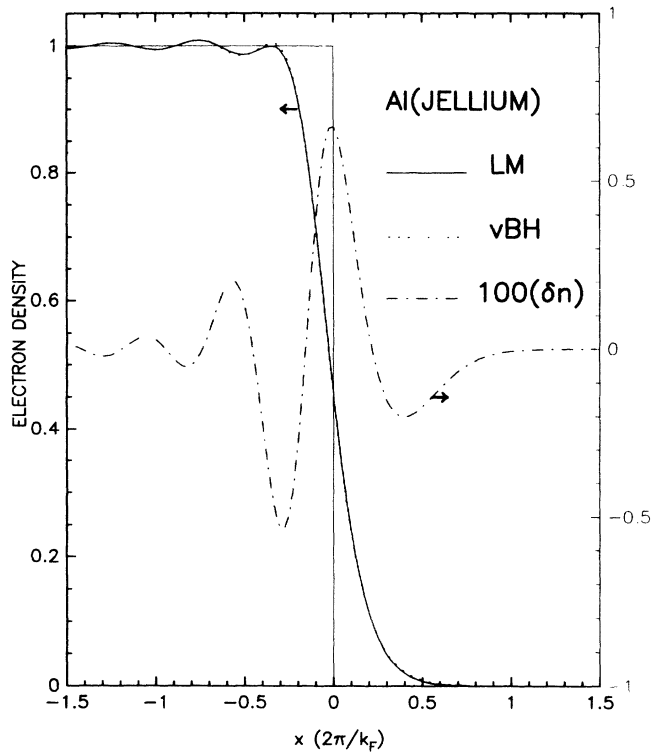


FIG. 5. The charge-density profile for a jellium surface with $r_s = 2.07$. Also plotted is the difference in density distributions, $\delta n = n^{nl, LM} - n^{LDA, vBH}$, times 100. All densities are in units of \bar{n} , which is the bulk average of $n(r)$.

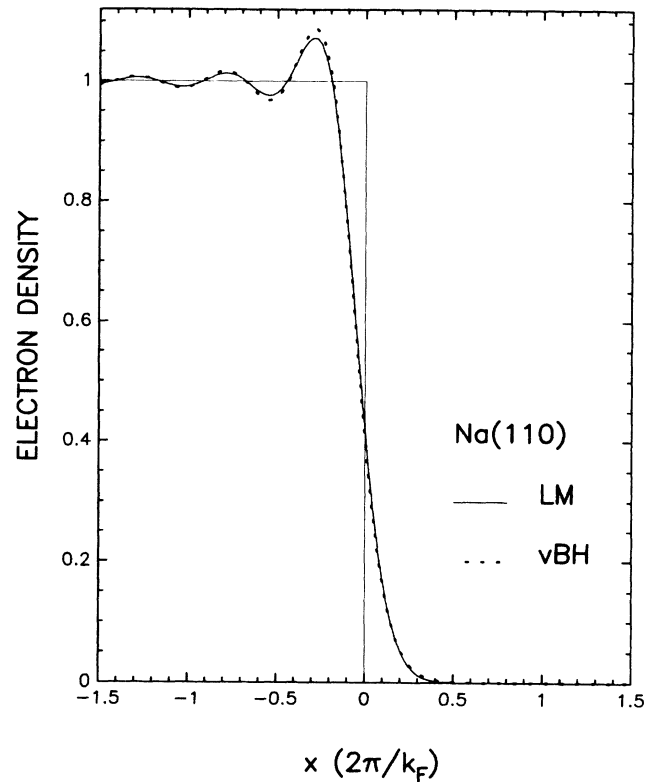


FIG. 7. Same as in Fig. 5, but for the real surface of Na [bcc (110) face, $C = 0.15$ eV].

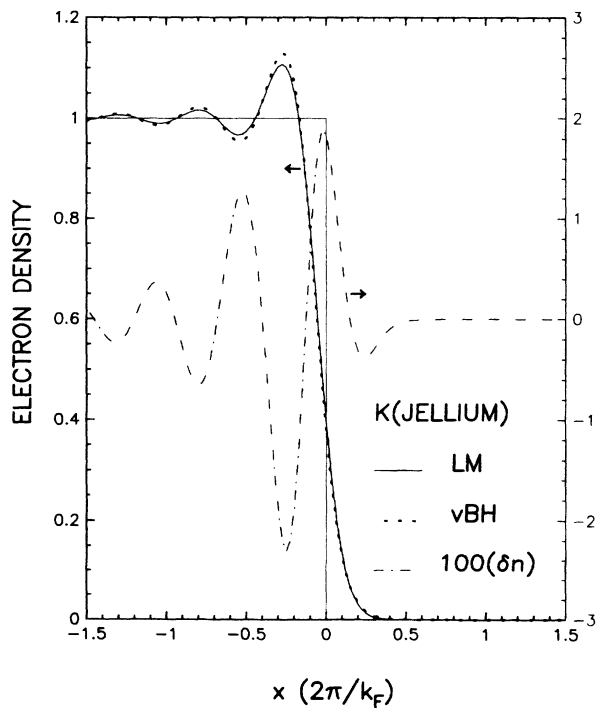


FIG. 6. Same as in Fig. 5, but for a jellium surface with $r_s = 4.96$.

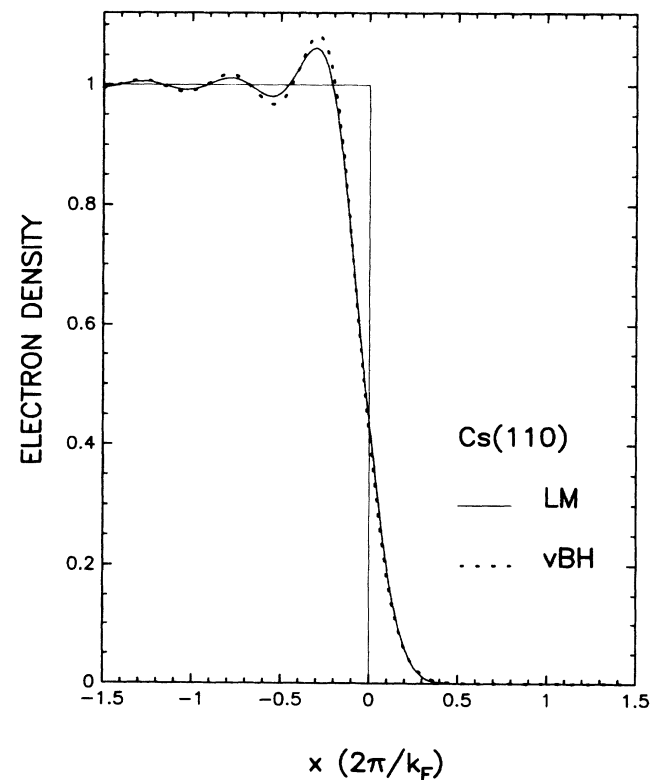


FIG. 8. Same as in Fig. 5, but for the real surface of Cs [bcc (110) face, $C = 1.05$ eV].

Another physical quantity of high current interest is the position of the image plane for a given surface. This quantity is just the location of the centroid of excess charge in the presence of a weak perpendicular electric field. It has been calculated by Lang and Kohn within the LDA.¹⁹ The recent development of the inverse photoemission technique and measurements of image-state properties necessitate more precise information on the position of the image plane,^{35–37} and several new but controversial calculations have appeared which include a nonlocal potential whose behavior is imagelike at large distances.^{29,32,33,38} In the work of Ossicini *et al.*²⁹ the nonlocal corrections to the one-particle potential and charge-density profile behave oppositely to our LM corrections, and the centroid of the induced charge moves slightly toward the jellium edge.³³ Therefore we expect that the LM correction should shift the centroid slightly *away* from the jellium edge. Serena, Soler, and Garcia³² have grafted the image-potential limit onto the LDA potential, and thereby obtained a small shift of the centroid *toward* the jellium edge. A similar shift might be expected if this limit were grafted onto the LM potential. While the nonlocal effects on the centroid of excess charge may be very small, the discrete-lattice effects represented by our potential $C_m \Theta(-x)$ could be important. In a future work we plan to present a calculation of the image-plane position using a procedure which remedies the incorrect behavior of the LM potential far away from the surface.

C. Surface energy

Again, we consider only the most densely packed surfaces of the seven simple metals. The results are summarized in Tables I–III.

The total surface energy contains five terms:^{16,17}

$$\sigma[n] = \sigma_s[n] + \sigma_{xc}[n] + \sigma_{es}[n] + \sigma_{ps}[n] + \sigma_{cl}, \quad (3.1)$$

where the first three terms represent the kinetic, exchange-correlation, and electrostatic energy contributions, respectively. When the variational parameter C is set to zero, the sum of those three terms is the jellium surface energy. The last two terms, the pseudopotential energy and the cleavage energy, arise when the ion-lattice model is used.

Table I lists the surface energies within the jellium

model (column 6). The two values in parentheses are from a previous estimate³⁹ which added the LM nonlocal correction in the linear potential model⁴ to the Lang-Kohn local value. Clearly these estimated values are quite a bit lower than those from the present self-consistent calculations. We also show results from the original calculation of Lang and Kohn¹⁷ within the LDA (Wigner interpolation formula for the exchange and correlation), LDA results from the more accurate Vosko-Wilk-Nusair (VWN) formula,⁴⁰ the RPA-based LDA results (vBH), as well as the results from the FHNC variational treatment of the ground-state wave function.²⁵ The nonlocal exchange-correlation contribution systematically increases the surface energy, an expected result.^{4,22} In contrast, the nonlocal exchange-correlation functional developed by Gunnarsson and Jones³⁰ gives *negative* corrections to the LDA surface energy.^{29,34} The figures in the column marked VWN should probably be considered close to the exact LDA values. The vBH column, which is the random-phase approximation to the LDA, was included because it represents the starting point for the LM approximation, which was entirely within the RPA.

The FHNC surface energies tend to be significantly higher than the LM surface energies. According to the analysis of Krotscheck and Kohn,⁴¹ the extra surface energy in the FHNC calculation arises from effects that are not only beyond the LDA, but also beyond the RPA, and thus inaccessible to the LM functional. Because this effect depends so sensitively upon short-ranged correlations, Krotscheck and Kohn were rather cautious in their claims for its size. The FHNC surface energies are further discussed in Appendix A.

In Table II, we give the total surface energy and two of its components for each of the seven elements within the ion-lattice model, for both $C=0$ and $C=C_m$. (The values of C_m for the last four elements are somewhat different from those found in Ref. 16). As first pointed out by Perdew and Monnier,¹⁵ surface energies drastically different from those of Lang and Kohn can be obtained when the discrete-lattice effects on the electron density are not weak; for Pb this effect may even reduce the surface energy by a factor of 2.

In Table III, we compare surface energies from the present calculation with those from other calculations and from experiment. Several observations can be made

TABLE I. Surface energies obtained in the present work for the jellium model in the LDA (VWN, column 4), the RPA-based LDA (vBH, column 5), and with nonlocal effects (LM, column 6). Results from Lang and Kohn (LK, Ref. 17), and Krotscheck *et al.* (FHNC, Ref. 25) are also shown. All surface energies are given in ergs/cm². Values in parentheses are *estimates* of the LM surface energy from Ref. 39.

r_s	Metal	LK	VWN	vBH	LM	FHNC
2.07	Al	-730	-602	-552	-484 (-645)	-222
2.30	Pb	-184	-101	-60	-9	181
3.28	Li	210	220	239	260	360
3.99	Na	160	164	176	189 (179)	261
4.96	K	100	100	106	114	159
5.23	Rb	85	87	93	100	
5.63	Cs	70	71	73	82	

TABLE II. The total surface energy σ obtained using LM, and two contributing components, the exchange-correlation part σ_{xc} and the pseudopotential part σ_{ps} , for the most densely packed faces of the seven simple metals (in units of ergs/cm²). In columns 5 and 6 we show values in the LDA (VWN) and the RPA-based LDA (vBH).

r_s	Metal	Face	C_m (eV)	σ_{xc}^{VWN}	σ_{xc}^{vBH}	σ_{xc}^{LM}	σ_{ps}	σ
2.07	Al fcc	(111)	0.0	2955	2989	3026	1025	949
			-1.9	2573	2602	2619	848	848
2.30	Pb fcc	(111)	0.0	2014	2041	2071	909	1297
			-6.3	1109	1121	1082	-322	659
3.28	Li bcc	(110)	0.0	546	557	574	109	428
			-1.1	455	462	472	74	407
3.99	Na bcc	(110)	0.0	262	268	280	35	257
			0.15	271	277	291	34	256
4.96	K bcc	(110)	0.0	113	116	125	21	153
			0.25	124	127	137	19	152
5.23	Rb bcc	(110)	0.0	92	94	102	18	132
			0.9	129	133	143	-5	122
5.63	Cs bcc	(110)	0.0	69	70	77	17	110
			1.05	107	111	120	-12	97

from this table. First, compare the $C=0$ calculations: the LM results (which include nonlocal effects within density-functional theory) and the results from the FHNC variational method are both higher than the LDA (VWN) results. The difference arises only in size of the increase. Second, compare the $C=C_m$ calculations: the LM results are in better agreement with experiment than the MP results at higher densities, while the MP results are slightly better at lower densities.

Perdew and Wang have proposed generalized gradient approximations which are often more accurate than LM for the exchange⁴² and correlation⁴³ energies, taken separately; it should be noted that there exist new results for the proper separation of exchange and correlation.⁴⁴ For the surface exchange-correlation energy, however, it is essential to treat exchange and correlation *together* and in the same way, since the strong nonlocalities of each tend to cancel.²⁰⁻²² Thus we do not use the Perdew-Wang functionals here; elsewhere¹³ they have been found to

reduce the LDA surface exchange-correlation energies by about 10%.

D. Work function

Following Eq. (4.5) of Monnier and Perdew,¹⁶ we obtain the work functions with the LM nonlocal functional included self-consistently. The results are shown in Table IV. Also shown are the results from other methods. In comparison with the LK work function, the LM work function is systematically larger. The major part of this difference results from replacement of the Wigner interpolation formula by the vBH parametrization for the LDA. The actual gradient terms in the LM scheme change the work-function amount to at most 30% of the change, and often much less. Nearly all the work functions in Table IV have been calculated from the equation¹⁶

TABLE III. Comparison of surface energies (in units of ergs/cm²). In the treatment of discrete-lattice effects, the FHNC approach is similar to the perturbative approach of LK and VWN, while SFW (Ref. 24) is similar to the variational approach of MP (Ref. 16) and the present work (LM).

r_s	Metal	Face	LK ^a	VWN ^a	MP	vBH ^b	LM ^b	SFW	FHNC	Expt. ^c
2.07	Al fcc	(111)	730	841	795	886/800	949/848	977	1323	965-1170
2.30	Pb fcc	(111)	1140	1185	456	1213/613	1297/659	1118	1737	593-690
3.28	Li bcc	(110)	380	402	392	404/388	428/407	465	553	470-522
3.99	Na bcc	(110)	230	237	247	247/246	257/256	264	318	220-275
4.96	K bcc	(110)	140	139	148	147/146	153/152	124	188	125-145
5.23	Rb bcc	(110)	120	121	117	131/117	132/122	107	119	95-117
5.63	Cs bcc	(110)	100	100	93	110/93	110/97	92		80-95

^aData for $C=0$.

^bData given in the form A/B , where A is the value for $C=0$ and B for $C=C_m$.

^cData from Ref. 24.

TABLE IV. Comparison of work functions (in units of eV). All work functions except those of LK were computed from Eq. (3.2).

r_s	Metal	Face	LK ^a	VWN ^b	MP	vBH ^a	LM ^a	SFW	Expt. ^c
2.07	Al fcc	(111)	3.87/4.05	3.79	4.0	4.22/4.38	4.12/4.26	3.6	4.19
2.30	Pb fcc	(111)	3.80/3.85	3.71	3.7	4.14/4.12	4.06/4.05	5.9	4.01
3.28	Li bcc	(110)	3.37/3.55	3.25	3.5	3.66/3.78	3.63/3.75	3.6	3.1
3.99	Na bcc	(110)	3.06/3.10	2.93	3.3	3.32/3.39	3.32/3.39	2.9	2.7
4.96	K bcc	(110)	2.74/2.75	2.57	2.9	2.94/3.07	2.95/3.09	2.7	2.39
5.23	Rb bcc	(110)	2.63/2.20	2.48	2.9	2.84/2.84	2.87/2.88	2.2	2.21
5.63	Cs bcc	(110)	2.49/2.25	2.37	2.8	2.72/2.73	2.74/2.78	2.1	2.12

^aData given in the form A/B , where A is the value for jellium and B for real metals.

^bData for jellium only.

^cData from Ref. 25.

$$W = \Delta\phi - \varepsilon_F(\bar{n}) - \mu_{xc}(\bar{n}) - \langle \delta v \rangle_{av}, \quad (3.2)$$

where $\Delta\phi$ is the surface electrostatic dipole barrier, $\varepsilon_F(\bar{n})$ is the free-electron Fermi energy, $\mu_{xc}(\bar{n})$ is the bulk exchange-correlation potential, and $\langle \delta v \rangle_{av}$ is the bulk average of the discrete-lattice potential. For jellium (3.2) is exact, but for real metals it is only approximate. A more accurate formula for variational descriptions of real-metal surfaces is the change-in-self-consistent-field (Δ SCF) expression⁴⁵

$$W = d\sigma/d\Sigma|_{\Sigma=0}, \quad (3.3)$$

the derivative of the surface energy σ with respect to the charge density Σ . Because (3.3) requires more laborious calculation than (3.2), it has not been employed in Table IV, except in the LK calculations for real metals.

IV. SUMMARY

A fully self-consistent calculation of electron densities and energies at planar metallic surfaces has been presented within density-functional theory using the Langreth-Mehl nonlocal functional. The main effects from the LM correction are a systematic decrease in the density oscillation near the surface region, and also a systematic increase in the surface energy and the work function.

ACKNOWLEDGMENTS

This work was completed while one of us (D.C.L.) visited Chalmers University of Technology; he thanks Chalmers University, NORDITA, and The Swedish National Research Council for financial support, and B. Lundqvist, his colleagues, and staff for scientific support and hospitality. We thank Z. X. Shen for some help at the initial stages of this work, Y. Wang for checks on some of the calculations, and E. Krotscheck for unpublished numerical results and comments on the manuscript. This work was supported in part by the National Science Foundation under Grants No. DMR-83-04210 and No. DMR-88-01027 (D.C.L.) and No. DMR-84-20964 (J.P.P.).

APPENDIX A: COMMENTS ON MANY-BODY-WAVE-FUNCTION CALCULATIONS FOR JELLIUM SURFACES

Correlated wave functions for jellium surfaces have been constructed by Sun, Farjam, and Woo^{23,24} (SFW)

and by Krotscheck, Kohn, and Qian^{25,41} (KKQ). The KKQ surface energy is obtained essentially from the expectation value of the Hamiltonian, and has been chosen in Table I as the standard against which to measure density-functional approximations. SFW used their correlated wave function only to evaluate the expectation values of one-body operators; they treated the electron-electron interaction via another density-functional model.

The difference $\sigma^{\text{FHNC}} - \sigma^{\text{VWN}}$ between the FHNC and local-density (VWN) values of the surface energy is then our best estimate of the contribution from the nonlocality of the exchange-correlation energy. For six of the seven real-metal r_s values considered by KKQ, we find $\sigma^{\text{FHNC}} - \sigma^{\text{VWN}} \approx (1520 \text{ ergs/cm}^2)/r_s^2$. The sole exception is the value for $r_s = 5.23$, which is 3 or 4 times smaller than expected. Krotscheck and Kohn⁴¹ omitted this anomalous (poorly covered) value in their discussion of the physics behind their results, and we have also omitted it in Table I.

KKQ used the Talman-Shadwick procedure⁴⁶ to solve the jellium surface problem essentially exactly at the exchange-only (Hartree-Fock) level. Their Hartree-Fock surface energies σ^{HF} have been reported by Krotscheck and Kohn.⁴¹ We have plotted these values onto Fig. 2 of Sahni and Ma,⁴⁷ which displays a rigorous variational upper bound to the Hartree-Fock surface energy as a function of r_s . The KKQ results fall near and a little below the bound (not shown here), as expected. From this, we conclude that the KKQ calculation is correct at the Hartree-Fock level.

The KKQ surface energies are surprisingly large; in fact, their surface correlation energies $\sigma_c = \sigma^{\text{FHNC}} - \sigma^{\text{HF}}$ are 4 or 5 times bigger than the LDA surface correlation energies. It is still not absolutely clear whether these large surface correlation energies are real or merely an artifact of the variational calculation. No hint of a large positive correction to the total LDA surface energy can be found in a comparison⁴⁸ between detailed real-metal calculations and experiment. However, we offer in support of the KKQ calculation an oversimplified, "back-of-the-envelope" model which predicts their surface correlation energies to within about 10%

Start with a uniform jellium of density $3/4\pi r_s^3$, in which the correlation energy per electron is $\varepsilon_c(r_s)$. Break it up into separated neutral "jelly atoms." Each jelly atom is a sphere of positive charge of radius r_s and density $3/4\pi r_s^3$, neutralized by a *single* electron. The correla-

tion energy change per electron is $-\varepsilon_c(r_s)$, and the surface area created per sphere is $4\pi r_s^2$. In the spirit of Ref. 31, the surface correlation energy is thus

$$\sigma_c \approx -\varepsilon_c^{\text{FHNC}}(r_s)/4\pi r_s^2. \quad (\text{A1})$$

Table V shows that Eq. (A1) successfully “explains” the KKQ values of the surface correlation energy, from an elementary perspective. Of course, the high level of agreement between the left- and right-hand sides of Eq. (A1) is probably fortuitous.

KKQ have also reported FHNC work functions for jellium. Their work functions are also surprisingly high, being as much as 1.1 eV bigger than the LDA work functions. We tentatively attribute this to the fact that they used a slab of thickness $14r_s a_0$ in place of a semi-infinite jellium.

Consider three different expressions^{16,47,49} for the work function of jellium which would be equal within any self-consistent Kohn-Sham calculation in the limit of large slab thickness:

$$W^{\text{Koopmans}} = \phi(\infty) - \phi(\text{center}) - [\varepsilon_F(\bar{n}) + \mu_{\text{xc}}(\bar{n})], \quad (\text{A2})$$

$$W^{\text{DPASCF}} = \phi(\infty) - \phi(\text{edge}) - [\frac{3}{5}\varepsilon_F(\bar{n}) + \varepsilon_{\text{xc}}(\bar{n})], \quad (\text{A3})$$

$$W_s = v_{\text{eff}}(\infty) - v_{\text{eff}}(\text{center}) - \varepsilon_F(\bar{n}). \quad (\text{A4})$$

Here, $\phi(x)$ is the electrostatic potential of Eq. (2.4), evaluated far outside the jellium slab, or at its edge, or at its center. $\varepsilon_F(\bar{n}) = (3\pi^2\bar{n})^{2/3}$ is the free-electron Fermi energy, and $\mu_{\text{xc}}(\bar{n}) = \partial[\bar{n}\varepsilon_{\text{xc}}(\bar{n})]/\partial\bar{n}$ is the exchange-correlation contribution to the chemical potential. KKQ used only Eq. (A2) in their evaluation of the work function. We have evaluated all three expressions using data from Figs. 8–10 and Table VII of KKQ. The results, displayed in our Table VI, show that different expressions yield significantly different values. Perhaps the KKQ slab is not thick enough to simulate a semi-infinite jellium in work-function calculations with Eq. (A2).

Equations (A2)–(A4) are not equal to the work function of a slab, except in the limit of large thickness. From Appendix B of Ref. 45, the correct expression for the work function of a slab of *any* thickness is

TABLE V. Comparison between the FHNC surface correlation energy (Refs. 25 and 41) and the prediction of Eq. (A1). All surface energies are given in ergs/cm². The FHNC correlation energy per electron of the uniform gas, $\varepsilon_c^{\text{FHNC}}$, is taken from Ref. 25. The LDA (VWN) surface correlation energies are shown for comparison.

r_s	$-\varepsilon_c^{\text{FHNC}}/4\pi r_s^2$	σ_c^{FHNC}	σ_c^{LDA}
2.07	1158	1051	283
2.30	886	855	208
2.66	612	598	135
3.28	357	355	72
3.99	214	221	39
4.96	121	124	20

TABLE VI. Work function evaluated from Eqs. (A2)–(A4), using data calculated by Krotscheck, Kohn, and Qian (KKQ) for a jellium slab of thickness $14r_s a_0$. These three expressions should agree in the limit of infinite thickness. For $r_s = 2.07$, we show exchange-only (x) as well as -correlated (xc) values. Values in parentheses are from Table V of KKQ. All work functions are in eV.

Method	r_s	Eq. (A2)	Eq. (A3)	Eq. (A4)
x	2.07	3.75	2.68	2.75
xc	2.07	4.80 (4.90)	4.10	2.10
xc	4.96	2.82 (2.83)	2.71	1.74

TABLE VII. Work function for a jellium slab of thickness d , evaluated from Eq. (A5) using KKQ data provided by Krotscheck. All work functions are in eV.

r_s	$d/r_s a_0$	W
2.07	10	3.37
	12	3.42
	14	3.39
2.30	10	3.30
	12	3.36
	14	3.35
3.28	10	2.84
	12	2.90
	14	2.92
3.99	10	2.53
	12	2.59
	14	2.61
4.96	10	2.22
	12	2.25
	14	2.26
5.23	10	2.14
	12	2.15
	14	2.20

TABLE VIII. Sensitivity of the nonlocal surface energies (ergs/cm²) to the value of f defined in Eq. (2.9). Column 4 gives the exchange-correlation component, column 5 gives the jellium total, and column 6 gives the total value. In all cases, $C = 0$.

r_s	Metal	f	σ_{xc}	σ_{jellium}	σ
2.07	Al	0.17	3026	−484	949
		0.15	3046	−454	975
3.99	Na	0.17	280	189	257
		0.15	283	195	263
5.63	Cs	0.17	77	82	110
		0.15	78	84	114

$$W = v_{\text{eff}}(\infty) - \epsilon^{\text{HO}}, \quad (\text{A5})$$

where ϵ^{HO} is the highest occupied Kohn-Sham orbital energy. Equation (A5) yields the work function of a slab because the slab is infinite in dimensions parallel to the surface, and so the electronic relaxation effects after removal of one electron are infinitesimal.

Since the KKQ slab is thick enough to produce Hartree-Fock-level surface energies in agreement with those of a semi-infinite jellium, it *may* also be thick enough to yield the work function of the correlated semi-infinite jellium surface. In order to test this possibility, we have evaluated Eq. (A5) as a function of slab thickness d in Table VII, using KKQ data kindly provided by Krotscheck. The resulting work functions for $d = 14r_0$ lie about 0.3 eV *lower* than the LDA (VWN) work functions for semi-infinite jellium (Table IV). Although it is not clear how to extrapolate these results to $d = \infty$, they do suggest that the work functions reported in Table V of

KKQ may be overestimated by 1 eV or more, due to the fact that Eq. (A2) is unsuitable for thin films.

APPENDIX B: SENSITIVITY TO f

Here we present calculations showing the sensitivity of our results to the value of f , for the range between 0.15 and 0.17 suggested by LM. The results are shown in Table VIII. We remark that although the changes in the total surface energy are not large, the percentage change in the quantity specifically under consideration, that is, the nonlocal component of the exchange-correlation energy, is significant ($\sim 20\%$). This is because the nonlocal component of the surface correlation energy, which depends directly on f , is nearly canceled by the nonlocal component of the surface exchange energy, which does not, thus leaving a small denominator with which to calculate percentages.

*Present address: Department of Chemistry, University of California, Santa Barbara, CA 93106.

¹P. Hohenberg and W. Kohn, Phys. Rev. **136**, B864 (1964).

²W. Kohn and L. J. Sham, Phys. Rev. **140**, A1333 (1965).

³D. C. Langreth and M. J. Mehl, Phys. Rev. Lett. **47**, 446 (1981).

⁴D. C. Langreth and M. J. Mehl, Phys. Rev. B **28**, 1809 (1983); **B 29**, 2310(E) (1984).

⁵D. C. Langreth and J. P. Perdew, Phys. Rev. B **21**, 5469 (1980).

⁶A. Savin, U. Wedig, H. Preuss, and H. Stoll, Phys. Rev. Lett. **53**, 2087 (1984).

⁷F. W. Kutzler and G. S. Painter, Phys. Rev. Lett. **59**, 1285 (1987).

⁸F. W. Kutzler and G. S. Painter, Phys. Rev. B **37**, 2850 (1988).

⁹M. R. Norman and D. D. Koelling, Phys. Rev. B **28**, 4357 (1983); P. Bagno, O. Jepsen, and O. Gunnarsson, *ibid.* **40**, 1997 (1989).

¹⁰U. von Barth, in *The Electronic Structure of Complex Systems*, edited by P. Phariseau and W. Temmerman (Plenum, New York, 1984).

¹¹U. von Barth and A. C. Pedroza, Phys. Scr. **32**, 353 (1985).

¹²A.-R. E. Mohammed and V. Sahni, Phys. Rev. B **31**, 4879 (1985).

¹³J. P. Perdew, M. K. Harbola, and V. Sahni, in *Condensed Matter Theories, Vol. 3*, edited by J. Arponen, R. F. Bishop, and M. Manninen (Plenum, New York, 1988).

¹⁴C. D. Hu and D. C. Langreth, Phys. Scr. **32**, 391 (1985); erratum (to be published).

¹⁵J. P. Perdew and R. Monnier, Phys. Rev. Lett. **37**, 1286 (1976).

¹⁶R. Monnier and J. P. Perdew, Phys. Rev. B **17**, 2595 (1978); **B 22**, 1124(E) (1980).

¹⁷N. D. Lang and W. Kohn, Phys. Rev. B **1**, 4555 (1970).

¹⁸N. D. Lang and W. Kohn, Phys. Rev. B **3**, 1215 (1971).

¹⁹N. D. Lang and W. Kohn, Phys. Rev. B **7**, 3541 (1973).

²⁰D. C. Langreth and J. P. Perdew, Solid State Commun. **17**, 1425 (1975).

²¹D. C. Langreth and J. P. Perdew, Phys. Rev. B **15**, 2884

(1977).

²²J. P. Perdew, D. C. Langreth, and V. Sahni, Phys. Rev. Lett. **38**, 1030 (1977).

²³X. Sun, T. Li, M. Farjam, and C.-W. Woo, Phys. Rev. B **27**, 3913 (1983).

²⁴X. Sun, M. Farjam, and C.-W. Woo, Phys. Rev. B **28**, 5599 (1983).

²⁵E. Krotscheck, W. Kohn, and G.-X. Qian, Phys. Rev. B **32**, 5693 (1985).

²⁶E. P. Wigner, Phys. Rev. **46**, 1002 (1934).

²⁷U. von Barth and L. J. Hedin, J. Phys. C **5**, 1629 (1972).

²⁸J. Herman, J. P. van Dyke, and I. B. Ortenburger, Phys. Rev. Lett. **22**, 807 (1969).

²⁹S. Ossicini, C. M. Bertoni, and P. Gies, Surf. Sci. **178**, 244 (1986); A. G. Eguiluz and W. Hanke, Phys. Rev. B **39**, 10433 (1989).

³⁰O. Gunnarsson and R. O. Jones, Phys. Scr. **21**, 394 (1980).

³¹J. P. Perdew, Phys. Rev. B **37**, 6175 (1988).

³²P. A. Serena, J. M. Soler, and N. Garcia, Phys. Rev. B **34**, 6767 (1986).

³³S. Ossicini, F. Finocchi, and C. M. Bertoni, Surf. Sci. **189/190**, 776 (1987).

³⁴E. Chacón and P. Tarazona, Phys. Rev. B **37**, 4020 (1988).

³⁵A. Liebsch, Phys. Rev. Lett. **54**, 67 (1985).

³⁶M. Weinert, S. L. Hulbert, and P. D. Johnson, Phys. Rev. Lett. **55**, 2055 (1985).

³⁷N. V. Smith, Rep. Prog. Phys. **151**, 1227 (1988).

³⁸P. Gies, J. Phys. C **19**, L209 (1986).

³⁹M. Rasolt and D. J. W. Geldart, Phys. Rev. B **34**, 1325 (1986).

⁴⁰S. H. Vosko, L. Wilk, and M. Nusair, Can. J. Phys. **58**, 1200 (1980).

⁴¹E. Krotscheck and W. Kohn, Phys. Rev. Lett. **57**, 862 (1986).

⁴²J. P. Perdew and Y. Wang, Phys. Rev. B **33**, 8800 (1986); **B 40**, 3399(E) (1989).

⁴³J. P. Perdew, Phys. Rev. B **33**, 8822 (1986); **B 34**, 7406(E) (1986).

⁴⁴D. C. Langreth and S. H. Vosko, in *Density Functional Theory of Many-Fermion Systems*, edited by S. B. Trickey (Academic,

- Orlando, 1989).
- ⁴⁵R. Monnier, J. P. Perdew, D. C. Langreth, and J. W. Wilkins, *Phys. Rev. B* **18**, 656 (1978).
- ⁴⁶J. D. Talman and W. F. Shadwick, *Phys. Rev. A* **14**, 36 (1976).
- ⁴⁷V. Sahni and C. Q. Ma, *Phys. Rev. B* **22**, 5987 (1980).
- ⁴⁸K.-P. Bohnen and S. Y. Tong, *Phys. Rev. B* **22**, 1806 (1980); K. M. Ho and K. P. Bohnen, *ibid.* **32**, 3446 (1985); R. Richter, J. R. Smith, and J. G. Gay, in *The Structure of Surfaces*, Vol. 2 of *Springer Series in Surface Sciences*, edited by M. A. Van Hove and S. Y. Tong (Springer, Berlin, 1985); J. R. Smith and A. Banerjea, *Phys. Rev. Lett.* **59**, 2451 (1987).
- ⁴⁹J. P. Perdew and V. Sahni, *Solid State Commun.* **30**, 87 (1979).